Integrated Sensing, Communications, and Powering for Statistical-QoS Provisioning Over 6G Massive-MIMO Mobile Networks Using FBC

Xi Zhang and Qixuan Zhu

Networking and Information Systems Laboratory
Department of Electrical and Computer Engineering, Texas A&M University, College Station, TX 77843, USA
E-mail: {*xizhang@ece.tamu.edu*, *qixuan@tamu.edu*}

ICC 2024 - IEEE International Conference on Communications | 978-1-7281-9054-9/24/$31.00 ©2024 IEEE | DOI: 10.1109/ICC51166.2024.10622315

***Abstract*—To satisfy the stringent quality-of-service (QoS) requirements of 6G mobile wireless networks on both channel state estimations and information transmissions, the *integrated sensing and communication (ISAC)* has been an enabling technique to sense and communicate by sharing the same frequency band and hardware. Simultaneous wireless information and power transfer (SWIPT) has also emerged to simultaneously deliver information and energy to a receiver. However, how to integrate ISAC with SWIPT to support the 6G traffic has imposed many new challenges not encountered before. To conquer these difficulties, in this paper we propose an integrated sensing, communications, and powering (ISACP) scheme for supporting statistical-QoS provisioning over 6G wireless networks using massive multiple-input and multiple-output (massive MIMO) communications. First, we establish system models for our ISACP scheme and define the Cramér-Rao bound and channel estimation distortion under our proposed ISACP scheme. Second, we develop the performance metrics of Cramér-Rao bound and channel estimation distortion to derive the capacity-distortion function to jointly measure the performance of integrated sensing, communication, and powering. Third, we integrate the capacity-distortion function with the finite blocklength coding (FBC) through deriving the ISACP-based ϵ-effective capacity to support the statistical delay and error-rate bounded QoS provisioning in 6G. Fourth, we maximize the energy-efficiency by controlling the optimal wireless power transfer for our ISACP scheme. Finally, we use numerical analyses to validate and evaluate our proposed ISACP scheme.**

***Index Terms*—6G, energy harvesting (EH), ISACP, capacity-distortion, massive MIMO, ϵ-effective capacity, statistical delay and error-rate bounded QoS, Cramér-Rao bound (CRB), FBC.**

I. Introduction

THE forthcoming 6G wireless networks are anticipated to accommodate a diverse range of communication traffics demanding stringent quality-of-service (QoS) requirements. One type of the dominant traffics in 6G wireless networks is the *massive ultra-reliable and low-latency communications* (mURLLC), such as *metaverse streaming* and *digital twins*, which require the short delay and low error probability for serving massive numbers of mobile users (MUs). To improve the QoS of mURLLC, the technique of *integrated sensing and communication (ISAC)* has been proposed to sense the wireless channel shared with sending the communication data in the same frequency band and hardware. For boosting the energy-efficiency via green communications over 6G wireless networks, simultaneous wireless information and power transfer (SWIPT) has also been developed to support energy consuming MUs by simultaneously conveying the *information* and *power*.

This work of Xi Zhang and Qixuan Zhu was supported in part by the U.S. National Science Foundation under Grants CCF-2142890, CCF-2008975, ECCS-1408601, and CNS-1205726, and the U.S. Air Force under Grant FA9453-15-C-0423.

Recent works have studied various ISAC schemes jointly considering power optimization problems. The work of [1] integrated ISAC systems with full-duplex sensing and half-duplex communication to maximize the sum rate over all MUs while minimizing the power consumption. The authors of [2] proposed a novel ISAC system to mitigate the overlapping of the radar and communication frequency bands through a micro base station (BS)'s full-duplex decode-and-forward relay mechanism to assist end-to-end communications. An integration of ISAC with uplink non-orthogonal multiple access system was studied by [3] via applying a signalling approach to enforce mutual interference cancellation between the radar and communication signals.

However, how to jointly optimize sensing, transmitting communication data, and powering for mURLLC traffics to guarantee the stringent QoS requirements remains an open problem. To overcome this challenge, in this paper we propose an integrated sensing, communications, and powering (ISACP) schemes for supporting statistical-QoS provisioning over 6G by using *massive multiple-input and multiple-output* (massive MIMO) communications. First, we establish the system models for the ISACP scheme by integrating the ISAC with SWIPT techniques to simultaneously sense the wireless channel, convey the information, and transfer the power. Second, we apply the finite blocklength coding (FBC) technique to transmit the ISACP signal and measure the performance metrics for the ISACP scheme using the Cramér-Rao bound, channel state estimation distortion. Third, we derive the capacity-distortion function and integrate it with the FBC scheme through the concept of the ISACP-based ϵ-effective capacity to support the statistical delay and error-rate bounded provisioning of the mURLLC traffic over 6G. In the end, we formulate an ISACP-based energy-efficiency maximization problem and solve this problem by optimizing the power splitting ratio between information signal and energy harvesting.

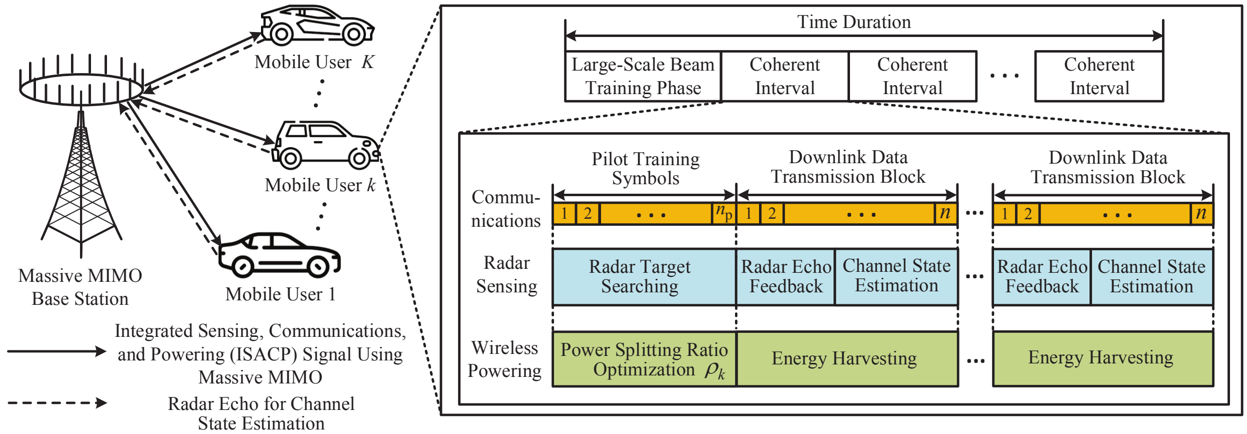

Fig. 1. The system architecture models of our proposed ISACP using massive MIMO, FBC, and SWIPT techniques (with FBC's finite blocklength equal to n and the uplink pilot signal sequence length equal to n_{p}) to perform: (1) the communications, including large-scale beam-training phase, uplink pilot training, and finite-blocklength downlink data transmission phases; (2) the radar sensing, including target searching, receiving echo feedback, and channel state estimation; and (3) the wireless powering, including the optimization for the power splitting ratio for assigning ρ_k portion of the total power to receive the signal and harvesting the rest $(1-\rho_k)$ portion of the total power.

The rest of this paper is organized as follows. Section II establishes the system models for our proposed ISACP-based architectures using massive-MIMO/FBC/SWIPT. Section III develops the performance metrics of the ISACP schemes. Section IV formulates an energy-efficiency maximization problem by optimizing the power splitting ratio. Section V validates and evaluates our developed ISACP schemes. This paper concludes with Section VI.

II. System Models for Our Proposed ISACP-Based Architectures Using Massive MIMO and FBC

As shown in Fig. 1, we consider a cellular network consisting of a massive MIMO BS and totally K moving targeted MUs, where the massive MIMO BS transmits the radar sensing and sends the downlink communication signals simultaneously to these K targeted MUs. Assume that there are M_T antennas on the BS and there are M_R antennas for each targeted MU, where $M_T \gg M_R$. The kth MU, $\forall k$, splits the received radio frequency (RF) signals from the massive MIMO BS into two parts with power splitting ratios ρ_k and $(1-\rho_k)$ for *receiving the information* and *energy harvesting*, respectively, where $0 < \rho_k < 1$.

In our proposed radar echo sensing scheme, each MU is considered as a scatterer to reflect the radar signal, and thus, the angle-of-arrival (AoA) and angle-of-departure (AoD) for each targeted MU are the same. The steering/response signal vector, denoted by $\mathbf{a}(M,\phi)$ for M antennas with AoA/AoD equal to ϕ, is defined as follows:

$$\mathbf{a}(M,\phi) \triangleq \left[1, e^{j\pi\sin(\phi)}, \dots, e^{j\pi(M-1)\sin(\phi)}\right]^{\intercal}, \quad (1)$$

where $(\cdot)^{\intercal}$ is the transpose operation. For the kth MU's radar-echo and radar-signal, let ϕ_k be the AoA and AoD of the kth MU (where AoA is equal to AoD for radar sensing). Define $\mathbf{S}^{\text{sen}} \in \mathbb{C}^{M_T \times M_T}$ as the target response matrix from the BS to the targeted MUs and reflected back to BS, which is given by

$$\mathbf{S}^{\text{sen}} = \sum_{k=1}^{K} \mu_k \mathbf{a}(M_T,\phi_k)\mathbf{a}(M_T,\phi_k)^{\intercal} \quad (2)$$

where μ_k is the amplitude of a complex value, characterizing both the signal attenuation and initial phase difference for the radar signal between the massive MIMO BS and the kth MU. Let B_k be the total power allocation for the kth MU's sensing and communication signal and define $\mathbf{B} \triangleq [B_1, B_2, \cdots, B_K]^{\intercal}$ as the power allocation vector for all K MUs. Let $\mathbf{x}_i(\mathbf{B}) \in \mathbb{C}^{M_T \times 1}$ be the transmitted signal under the power allocation vector $\mathbf{B}$ for the ith symbol, $\forall i \in \{1, \cdots, n\}$, from the massive MIMO BS to all K MUs. Since all MUs are energy harvesting devices, the kth MU, $\forall k$, uses ρ_k portion of the energy to receive information and harvests the rest $(1-\rho_k)$ portion of the energy. Denote by $\widetilde{\mathbf{B}} \triangleq [\rho_1 B_1, \rho_2 B_2, \cdots, \rho_K B_K]^{\intercal}$ the vector for the signal power after MUs' energy harvesting. After MUs' energy harvesting, the reflected radar echo signal for the ith symbol under the signal power vector $\widetilde{\mathbf{B}}$, denoted by $\mathbf{y}_i^{\text{sen}}(\widetilde{\mathbf{B}})$, received by the massive MIMO BS is given by

$$\mathbf{y}_i^{\text{sen}}(\widetilde{\mathbf{B}}) = \mathbf{S}^{\text{sen}}\mathbf{x}_i(\widetilde{\mathbf{B}}) + \mathbf{w}^{\text{sen}}, \ \forall i \in \{1, 2, \cdots n\} \quad (3)$$

where $\mathbf{x}_i(\widetilde{\mathbf{B}})$ can be obtained by replacing $\mathbf{B}$ in $\mathbf{x}_i(\mathbf{B})$ by $\widetilde{\mathbf{B}}$ and $\mathbf{w}^{\text{sen}} \in \mathbb{C}^{M_T \times 1}$ is additive white Gaussian noise (AWGN) at all M_T antennas deployed in the massive MIMO BS.

III. ISACP-Based Capacity-Distortion Function

A. The Cramér-Rao Bound for Radar Sensing

We propose to measure the performance of radar sensing by the *Cramér-Rao bound (CRB)* [4], which provides a lower bound on the variance of any unbiased estimator of a parameter. We develop CRB to measure the lower-bound for the variance of the estimated AoA/AoD of the kth MU, denoted by $\text{Var}[\widehat{\phi}_k|\rho_k B_k], \forall k$, under the signal power $\rho_k B_k$, and define the *Cramér-Rao bound*, denoted by $CRB\big(\widehat{\phi}_k, \rho_k B_k\big)$, as follows:

$$CRB\left(\widehat{\phi}_k, \rho_k B_k\right) \triangleq \inf\left\{\text{Var}\left[\widehat{\phi}_k \middle| \rho_k B_k\right]\right\}$$

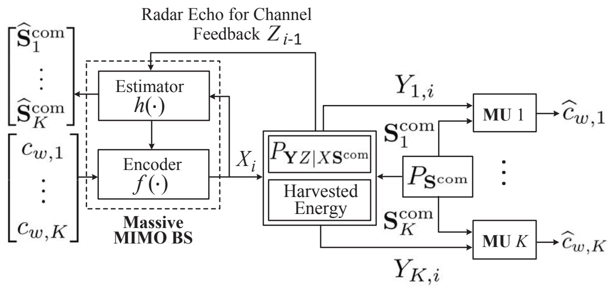

Fig. 2. The ISACP's encoding, decoding, channel estimation, and energy harvesting model at the ith channel use with $i = 1, 2, \ldots, n$ to transmit every message for each of K MUs, where n is FBC's codeword blocklength.

$$\triangleq \left(-\mathbb{E}\left[\frac{\partial^2 \log p(\mathbf{y}_i^{\text{sen}}(\widetilde{\mathbf{B}}); \phi_k)}{\partial \phi_k^2}\right]\right)^{-1}$$

$$\stackrel{(a)}{=} \frac{\sigma_w^2}{2|\mu_k|^2 n}\left\{\frac{\text{tr}\big(\mathbf{A}^H\mathbf{A}\mathbf{R}_\mathbf{X}\big)}{\text{tr}\Big(\dot{\mathbf{A}}^H\dot{\mathbf{A}}\mathbf{R}_\mathbf{X}\Big)\text{tr}\Big(\dot{\mathbf{A}}^H\dot{\mathbf{A}}\mathbf{R}_\mathbf{X}\Big) - \Big|\text{tr}\Big(\dot{\mathbf{A}}^H\mathbf{A}\mathbf{R}_\mathbf{X}\Big)\Big|^2}\right\} \tag{4}$$

where $p(\alpha;\beta)$ is the probability density function of α with β as a parameter, (a) is due to [5, Eq. (63)], the input signal matrix $\mathbf{X} \triangleq \mathbf{x}^n(\widetilde{\mathbf{B}}) \triangleq [\mathbf{x}_1(\widetilde{\mathbf{B}}), \cdots, \mathbf{x}_n(\widetilde{\mathbf{B}})] \in \mathbb{C}^{M_T \times n}$, where n is the number of symbols, $\mathbf{R}_\mathbf{X} \triangleq (1/n)\mathbf{X}\mathbf{X}^H$, σ_w^2 is the variance of AWGN, $\mathbf{A} \triangleq \mathbf{a}(M_T, \phi_k)\mathbf{a}(M_T, \phi_k)^\intercal$, $\dot{\mathbf{A}} \triangleq \partial\mathbf{A}/\partial\phi_k$, and $(\cdot)^H$ and $\text{tr}(\cdot)$ denote the conjugate transpose and the trace, respectively.

B. FBC Techniques to Support mURLLC Streaming

As shown in Fig. 2, the FBC supports mURLLC traffic by encoding the message with short packets to mitigate the transmission delay. We define an FBC scheme as follows.

Definition 1: We consider a wireless fading channel, which uses input blockcode set $\mathcal{X}$ and output blockcode set $\mathcal{Y}$. We define that an (n, W_k, ϵ_k)-code, $\forall k \in \{1, 2, \ldots, K\}$, for a state-dependent memoryless channel consists of [6, 7]:

- A message set $\mathcal{W}_k = \{c_{1,k}, \cdots, c_{W_k,k}\}$, $\forall k$, with the cardinality W_k and the message length equal to $\log_2(W_k)$ under FBC, see Figs. 1 and 2.
- A delayed feedback output set $\mathcal{Z}^{i-1}, \forall i \in \{1, \ldots, n\}$. An encoder is a function f: $\mathcal{W}_1 \times \cdots \times \mathcal{W}_K \times \mathcal{Z}^{i-1} \mapsto \mathcal{X}^n$, where $\mathcal{X}^n$ is the set of codewords with length n and $\mathcal{Z}^{i-1}$ is the set of $(i-1)$ feedback outputs.
- The channel state set $\mathcal{S}_k^{\text{com}}, \forall k$. At the receiver end, a decoder produces an estimate of the original message by observing the channel output, according to a function: $\mathcal{Y}^n \times \mathcal{S}_k^{\text{com}} \mapsto \widehat{\mathcal{W}}_k$, where $\mathcal{Y}^n$ is the set of received codewords with length n and $\widehat{\mathcal{W}}_k$ is an estimation of $\mathcal{W}_k$.
- The decoding-error probability, denoted by ϵ_k, is defined as $\epsilon_k \triangleq \frac{1}{W_k}\sum_{w=1}^{W_k} \Pr\{c_{w,k} \neq \widehat{c}_{w,k}\}$, where the message index $w \in \{1, \cdots, W_k\}$, a message $c_{w,k} \in \mathcal{W}_k$ and its estimated message $\widehat{c}_{w,k}$ received at MU k, with $\widehat{c}_{w,k} \in \widehat{\mathcal{W}}_k$.
- The channel state estimation function h: $\mathcal{X}^n \times \mathcal{Z}^n \mapsto \widehat{\mathcal{S}}_k^{\text{com}}$, where $\widehat{\mathcal{S}}_k^{\text{com}}$ is the estimation of $\mathcal{S}_k^{\text{com}}$ at the transmitter.

where usually $\epsilon_k > 0$ if $n < \infty$. ■

Thus, the triple-tuple (n, W_k, ϵ_k) defines the data source with the cardinality W_k which can successfully transmit the messages with a probability of success $(1-\epsilon_k)$ over n channel uses. In Fig. 2, Z_{i-1} is the channel feedback at the $(i-1)$th channel use. The channel input at the ith channel use is $X_i = f(W_1, \ldots, W_K, \mathbf{Z}^{i-1})$, $i \in \{1, 2, \cdots, n\}$, with the given encoding scheme $f(\cdot)$, where $\mathbf{Z}^{i-1} \in \mathcal{Z}^{i-1}$ is the sequence of channel feedback by the $(i-1)$th channel use. We define the communication channel state matrix for all MUs as $\mathbf{S}^{\text{com}} \triangleq [\mathbf{S}_1^{\text{com}}, \cdots, \mathbf{S}_K^{\text{com}}]^\intercal$, where $\mathbf{S}_k^{\text{com}} \in \mathcal{S}_k^{\text{com}}$ is the kth MU's communication channel state, the channel output sequence as $\mathbf{Y} \triangleq [Y_{1,i}, \cdots, Y_{K,i}]$, where the channel output at the ith channel use $Y_{k,i}$ is obtained from the state $\mathbf{S}_k^{\text{com}}$ and the input X_i using the transition law $P_{\mathbf{Y}Z|X\mathbf{S}^{\text{com}}}$, and $\widehat{\mathbf{S}}_k^{\text{com}} \in \widehat{\mathcal{S}}_k^{\text{com}}$.

C. The Channel State Estimation Distortion

We use s_k to represent the realization of any element in $\mathbf{S}_k^{\text{com}}$, and use $\hat{s}_k$ and $\hat{\mathbf{s}}_k^n$ to represent the estimation for s_k and $\mathbf{s}_k^n$, respectively, where $\mathbf{s}_k^n$ is the sequence of s_k over n channel uses. Define a function $d: \mathcal{S}_k^{\text{com}} \times \widehat{\mathcal{S}}_k^{\text{com}} \mapsto [0, \infty)$ as the channel state estimation distortion function. Using the mean squared error (MSE), we define the channel state estimation distortion of the ISACP scheme in the following definition.

Definition 2: The kth MU's *channel state estimation distortion*, denoted by $D_k(\rho_k B_k)$, of the ISACP scheme due to the *radar estimation distortion* under the power splitting ratio ρ_k and transmit power allocation B_k, is defined as follows [7]:

$$D_k(\rho_k B_k) \triangleq \mathbb{E}\Big[d\Big(\mathbf{s}_k^n, \hat{\mathbf{s}}_k^n\Big(\mathbf{x}^n(\widetilde{\mathbf{B}}), \mathbf{z}^{n-1}\Big)\Big)\Big]$$
$$\triangleq \frac{1}{n}\sum_{i=1}^{n}\mathbb{E}\left[\Big\|s_k - \hat{s}_k\Big(\mathbf{x}_i(\widetilde{\mathbf{B}}), z_{i-1}\Big)\Big\|_F^2\right] \leq D_{\text{a}} \tag{5}$$

where $\mathbf{x}^n(\widetilde{\mathbf{B}})$ is defined in the text following Eq. (4), $\mathbf{x}_i(\widetilde{\mathbf{B}})$ is specified in the text following Eq. (3), $\|\cdot\|_F$ is the Frobenius norm; $\mathbf{x}^n(\widetilde{\mathbf{B}}) \in \mathcal{X}^n$ and $\mathbf{z}^{n-1} \in \mathcal{Z}^{n-1}$ based on Definition 1; $\hat{\mathbf{s}}_k^n\Big(\mathbf{x}^n(\widetilde{\mathbf{B}}), \mathbf{z}^{n-1}\Big)$ and $\hat{s}_k\Big(\mathbf{x}_i(\widetilde{\mathbf{B}}), z_{i-1}\Big)$ are the channel state estimation sequence and function, respectively, defined in Definition 1; and D_{a} is the *achievable channel estimation distortion* if there exists a sequence of (n, W_k, ϵ_k)-codes defined in Definition 1 such that distortion $D_k(\rho_k B_k)$ defined by Eq. (5) satisfies:

$$\limsup_{n\to\infty}\{D_k(\rho_k B_k)\} \leq D_{\text{a}} \tag{6}$$

and the decoding-error probability ϵ_k defined in Definition 1 satisfies $\epsilon_k \triangleq \frac{1}{W_k}\sum_{w=1}^{W_k}\Pr\{c_{w,k} \neq \widehat{c}_{w,k}\} \to 0$ as $n \to \infty$. ■

D. Maximization for The Capacity-Distortion Function

To jointly measure the channel capacity and the channel state estimation distortion in ISACP, we employ the capacity-distortion function [7] to represent the tradeoff between the channel-capacity and the sensing distortion. Denoted by $c_k(x, \rho_k B_k)$ the *channel estimation cost function* for the kth MU under the signaling x and signal power $\rho_k B_k$. We define the capacity-distortion function [7, Eq. (3)], for the kth targeted MU, denoted by $C_k(\rho_k B_k, D_{\text{a}})$, as follows:

$$C_k(\rho_k B_k, D_{\text{a}}) = \sum_{m=(k-1)M_R+1}^{kM_R} \max_{\rho_k, P_X \in \mathcal{P}_{D_{\text{a}}}}\{I\left(X; Y\,|\mathbf{s}_m^{\text{com}}\right)\}$$

$$= \sum_{m=(k-1)M_R+1}^{kM_R} \log_2(1+\varphi_m(\rho_k B_k, D_{\text{a}})) \tag{7}$$

$$\text{s.t.: C1}: \; CRB\left(\widehat{\phi}_k, \rho_k B_k\right) \leq CRB_{\max}$$
$$\text{C2}: \; D_k(\rho_k B_k) = \sum\nolimits_{x\in\mathcal{X}} c_k(x, \rho_k B_k) P_X(x) \leq D_{\text{a}} \tag{8}$$
$$\text{C3}: \; \frac{1}{n}\sum\nolimits_{i=1}^{n} \mathbb{E}\left[b(X_i)\right] \leq \rho_k B_k$$

where $\mathcal{P}_{D_{\text{a}}} \triangleq \left\{P_X : \sum_{x\in\mathcal{X}} P_X(x) c_k^*(x, \rho_k B_k) \leq D_{\text{a}}\right\}$, where $c_k^*(x, \rho_k B_k)$ is the minimum $c_k(x, \rho_k B_k)$ that can be achieved for a given signaling $x \in \mathcal{X}$, $I(\cdot;\cdot|\cdot)$ is the conditional mutual information, $CRB\left(\widehat{\phi}_k, \rho_k B_k\right)$ is defined in Eq. (4), $CRB_{\max}$ is the maximum tolerable Cramér-Rao bound for estimating a targeted MU's AoA/AoD, and $b(X_i)$ is the transmit power allocation for X_i. In Eq. (7), $m \in \{1, 2, \cdots, KM_R\}$ is the index of antennas for all K MUs, where we assume that the mth antenna belongs to the kth MU, and $\varphi_m(\rho_k B_k, D_{\text{a}})$ is the received signal-to-noise ratio (SNR) on the mth antenna of all MUs, given by:

$$\varphi_m(\rho_k B_k, D_{\text{a}}) = \frac{\frac{\rho_k B_k}{M_T} \text{Var}\left[U_m(D_{\text{a}})\right]}{\text{Var}[\Omega_m]} \tag{9}$$

where Var$[\cdot]$ is the variance, $U_m(D_{\text{a}})$ is the received desired signal on the mth antenna of MUs under the achievable channel estimation distortion D_{a}, and Ω_m is the *effective additive noise* on the mth antenna of all MUs, including the AWGN noise and negligible inter-user interference.

IV. Maximization for Energy-Efficiency Under Our Developed ISACP Schemes

A. The ISACP-Based ϵ-Effective Capacity

The statistical delay-bounded QoS guarantees [8, 9] have been shown to be powerful in analyzing queuing behavior for the stochastic arrival and service processes over the time-varying wireless fading channels. The key statistical-QoS performance metric is the *effective capacity* which measures the maximum packet's constant arrival rate such that the given statistical *delay-bounded* QoS can be guaranteed. Based on the large deviation principle (LDP) [8], the queue-length process $Q_k(t)$ for the kth MU converges in distribution to a random variable $Q_k(\infty)$ such that

$$-\lim_{Q_{\text{th},k}\to\infty} \frac{\log(\Pr\{Q_k(\infty) > Q_{\text{th},k}\})}{Q_{\text{th},k}} = \theta_k \tag{10}$$

where $Q_{\text{th},k}$ is the queue length threshold (bound) and $\theta_k > 0$ is defined as the *QoS exponent* for MU k. The insights of Eq. (10) reveal that the probability of the queueing process exceeding a certain threshold $Q_{\text{th},k}$ decays exponentially fast at the rate of θ_k as the threshold $Q_{\text{th},k}$ increases and tends to infinity. As shown in [8], a smaller θ_k corresponds to a slower decay rate, which implies that the system can only provide a looser QoS guarantee, while a larger θ_k leads to a faster decay rate, which means that a more stringent QoS can be supported.

However, the conventional statistical-QoS theory modeled by Eq. (10) focuses only on the statistical delay-bounded QoS without considering the transmission reliability, which is thus not feasible to support mURLLC in our proposed ISACP scheme over 6G. To remedy these deficiencies, in this paper we propose to integrate the ISACP with the FBC-based effective-capacity theory to support *both* the statistical *delay* and *error-rate* bounded QoS provisioning. In particular, applying our derived ISACP channel-state estimation-distortion and capacity-distortion functions to derive the decoding error probability function, we develop and derive the new statistical QoS performance metric called: *ISACP-based ϵ-effective capacity* to guarantee *both* the statistical *delay* and *error-rate* bounded QoS provisioning for our proposed ISACP-based 6G wireless networks through the following definition.

Definition 3: For an (n, W_k, ϵ_k)-code, the *ISACP-based ϵ-effective capacity* (bits/sec/Hz), denoted by $EC_k(\theta_k, \epsilon_k(\rho_k B_k, D_{\text{a}}))$, as the function of the delay QoS exponent θ_k, ISACP's *achievable channel estimation distortion* D_{a} for the kth targeted MU, and FBC's decoding-error probability, denoted by $\epsilon_k(\rho_k B_k, D_{\text{a}})$, is defined as the maximum constant arrival rate for a given service process subject to *both* the statistical *delay* and *error-rate* bounded QoS requirements, which is derived as follows:

$$EC_k(\theta_k, \epsilon_k(\rho_k B_k, D_{\text{a}})) = -\frac{1}{n\theta_k}\log\Big\{\mathbb{E}_{r_k}[\epsilon_k(\rho_k B_k, D_{\text{a}})] + \mathbb{E}_{r_k}[1-\epsilon_k(\rho_k B_k, D_{\text{a}})]e^{-\theta_k \log_2(W_k)}\Big\} \tag{11}$$

where $\mathbb{E}_{r_k}\{\cdot\}$ denotes the expectation with respect to the random distance r_k between the kth MU and the BS, θ_k is derived in Eq. (10), and the decoding-error probability $\epsilon_k(\rho_k B_k, D_{\text{a}})$ defined in Definition 1, which measures the error-rate bounded QoS requirement, is derived by [6, Eq. (1)]:

$$\epsilon_k(\rho_k B_k, D_{\text{a}}) \approx Q\left(\frac{C_k(\rho_k B_k, D_{\text{a}}) - \frac{\log_2(W_k)}{n}}{\sqrt{V_k(\rho_k B_k, D_{\text{a}})/n}}\right) \tag{12}$$

where D_{a} is ISACP's *achievable channel estimation distortion* specified by Eqs. (5) and (6), $Q(\cdot)$ is the *Q*-function, $C_k(\rho_k B_k, D_{\text{a}})$ is the capacity-distortion function derived in Eq. (7), and $V_k(\rho_k B_k, D_{\text{a}})$ is the *channel dispersion* of the kth targeted MU, which is given as follows [6, Eq. (293)]:

$$V_k(\rho_k B_k, D_{\text{a}}) \approx \sum_{m=(k-1)M_R+1}^{kM_R} \left[1 - \frac{1}{(1+\varphi_m(\rho_k B_k, D_{\text{a}}))^2}\right] \tag{13}$$

where $\varphi_m(\rho_k B_k, D_{\text{a}})$ is the SNR derived by Eq. (9) as a function of D_{a} specified by Eqs. (5) and (6). ■

B. Maximizing The Energy-Efficiency For Our ISACP Schemes

Define the power splitting ratio vector, denoted by $\boldsymbol{\rho}$, for all K MUs as follows:

$$\boldsymbol{\rho} \triangleq [\rho_1, \rho_2, \cdots, \rho_K]^{\intercal}. \tag{14}$$

Denote by $B(\boldsymbol{\rho})$ the total power consumption (Joule/sec) for the ISACP-based massive MIMO communications system under the power splitting ratio vector $\boldsymbol{\rho}$, which is given by:

$$B(\boldsymbol{\rho}) = B_{\text{T}} + KB_{\text{R}} + \sum_{k=1}^{K} \rho_k B_k$$

$$-\sum_{k=1}^{K}(1-\rho_k)B_k-\sum_{k=1}^{K}\Gamma_k(\rho_k)-\sum_{k=1}^{K}\sum_{\substack{m=\\(k-1)M_R+1}}^{kM_R}\Omega_m \qquad (15)$$

where $B_{\rm T}$ is a constant signal processing circuit power consumption in the massive MIMO BS, $B_{\rm R}$ is a constant circuit power consumption of each MU, $\Gamma_k(\rho_k)$ is the energy harvested from the information signal at the kth MU given by:

$$\Gamma_k(\rho_k) = \sum_{m=(k-1)M_R+1}^{kM_R} \frac{\rho_k B_k}{M_T}{\rm Var}\left[U_m(D_{\rm a})\right], \qquad (16)$$

where $U_m(D_{\rm a})$ and Ω_m, respectively, are defined in the text following Eq. (9), and Ω_m represents the energy harvested from the effective additive noise by the mth antenna of MUs.

We define the overall *energy-efficiency* (bits/Joule/Hz), denoted by $\eta(\boldsymbol{\rho})$, for the ISACP-based massive MIMO communications system by a function of power splitting ratio vector $\boldsymbol{\rho}$ defined in Eq. (14) as the total number of bits successfully conveyed to all K MUs per Joule consumed energy under the *statistical delay and error-rate bounded QoS provisioning*, which is given by

$$\eta(\boldsymbol{\rho}) \triangleq \frac{\sum_{k=1}^{K} EC_k(\theta_k, \epsilon_k(\rho_k B_k, D_{\rm a}))}{B(\boldsymbol{\rho})} \qquad (17)$$

where $EC_k(\theta_k, \epsilon_k(\rho_k B_k, D_{\rm a}))$ is the kth MU's ϵ-effective capacity given by Eq. (11), and $B(\boldsymbol{\rho})$ is the total power consumption given by Eq. (15). Then, we maximize the energy-efficiency $\eta(\boldsymbol{\rho})$ as follows:

$$\max_{\boldsymbol{\rho}}\{\eta(\boldsymbol{\rho})\} \qquad (18)$$

$$\text{s.t.: C1}: \; CRB\left(\widehat{\phi}_k, \rho_k B_k\right) \le CRB_{\max}, \forall k$$

$$\text{C2}: \; D_k(\rho_k B_k) = \sum_{x\in\mathcal{X}} c_k(x, \rho_k B_k) P_X(x) \le D_{\rm a}, \forall k$$

$$\text{C3}: \; \frac{1}{n}\sum_{i=1}^{n} \mathbb{E}\left[b(X_i)\right]\rho_k \le B_k, \forall k,$$

where $CRB\left(\widehat{\phi}_k, \rho_k B_k\right)$ in C1 is defined in Eq. (4). Solving Eq. (18), we can obtain the optimal power splitting ratio vector, denoted by $\boldsymbol{\rho}^* \triangleq [\rho_1^*, \cdots, \rho_K^*]$, where $\rho_k^*, \forall k$, is the solution of Eqs. (19)-(20) presented at the bottom this page, where λ_1, λ_2, and λ_3 are the Lagrangian multipliers for the constraints C1, C2, and C3 in Eq. (18), respectively, $C\dot{R}B\left(\widehat{\phi}_k, \rho_k B_k\right) \triangleq \partial\left[CRB\left(\widehat{\phi}_k, \rho_k B_k\right)\right] \Big/ \partial\rho_k$, and $\dot{D}_k \triangleq \partial D_k(\rho_k B_k)/\partial\rho_k$.

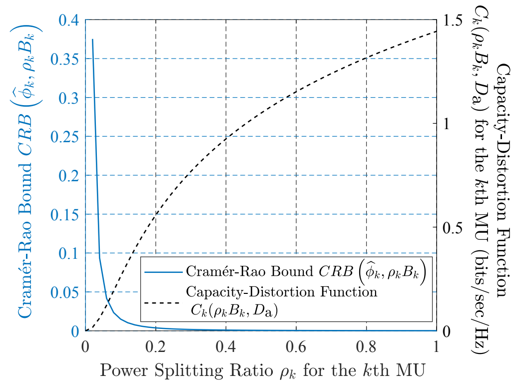

Fig. 3. Cramér-Rao bound $CRB\left(\widehat{\phi}_k, \rho_k B_k\right)$ and capacity-distortion function $C_k(\rho_k B_k, D_{\rm a})$ under different values of power splitting ratio ρ_k.

V. Performance Evaluations

Figure 3 plots both the Cramér-Rao bound $CRB\left(\widehat{\phi}_k, \rho_k B_k\right)$ and the capacity-distortion function $C_k(\rho_k B_k, D_{\rm a})$ under different values of power splitting ratio ρ_k for the kth MU. We set the number of antennas on the BS $M_T = 50$, total power allocation for the kth MU $B_k = 3$W, and the actual AoA/AoD for the kth MU $\phi_k = 30°$. Figure 3 shows that the Cramér-Rao bound decreases as the power splitting ratio ρ_k increases. This is because a larger ρ_k yields a larger power allocation for the integrated sensing and communication signal, and thus, yields a smaller variance for the targeted MU position sensing result. We can also observe from Fig. 3 that $C_k(\rho_k B_k, D_{\rm a})$ increases as the power splitting ratio ρ_k increases, because a larger power allocation for the integrated sensing and communication signal yields a larger ϵ-effective capacity. Figure 3 also shows that when the power splitting ratio ρ_k is 0.4, the Cramér-Rao bound approaches to zero, showing that increasing ρ_k after 0.4 cannot significantly improve the radar sensing results.

Figure 4 plots the ϵ-effective capacity in our proposed ISACP scheme against delay QoS exponent θ_k and power splitting ratio ρ_k for the kth MU, respectively. We set $M_T = 100$, number of antennas on MUs $M_R = 4$, $B_k = 2$W, and total number of MUs $K = 100$. We can observe from Fig. 4 that the ISACP-based ϵ-effective capacity is a monotonically decreasing function of the delay QoS exponent θ_k. This is because the θ_k measures the statistical delay QoS stringency, and thus, a channel with a looser delay QoS requirement can support a larger data arrival rate. We can observe from Fig. 4 that the ISACP-based ϵ-effective capacity is a monotonically

$$\frac{M_R\log_2(1+\varphi_m(\rho_k B_k, D_{\rm a})) - \frac{\log_2(W_k)}{n}}{(1+\varphi_m(\rho_k B_k, D_{\rm a}))^2} - \frac{1}{\log 2} = \sqrt{\frac{V_k(\rho_k B_k, D_{\rm a})}{n}}(1+\varphi_m(\rho_k B_k, D_{\rm a}))\frac{M_T\Psi(\rho_k){\rm Var}\left[\Omega_m\right]}{M_R B_k {\rm Var}\left[U_m(D_{\rm a})\right]}, \;\forall k \qquad (19)$$

where $k \in \{1, 2, \cdots, K\}$ and also

$$\Psi(\rho_k) = \frac{n\theta_k\left[\epsilon_k(\rho_k B_k, D_{\rm a}) + [1-\epsilon_k(\rho_k B_k, D_{\rm a})]e^{-\theta_k\log_2(W_k)}\right]}{\left(1-e^{-\theta_k\log_2(W_k)}\right)}$$
$$\times\left\{\sum_{k=1}^{K} EC_k(\theta_k, \epsilon_k(\rho_k B_k, D_{\rm a}))\frac{2B_k - \frac{B_k}{M_T}{\rm Var}[U_m(D_{\rm a})]}{B(\boldsymbol{\rho})} + \left(\lambda_1 B_k B(\boldsymbol{\rho}) + \lambda_2 C\dot{R}B\left(\widehat{\phi}_k, \rho_k B_k\right) + \lambda_3\dot{D}_k\right)B(\boldsymbol{\rho})\right\} \qquad (20)$$

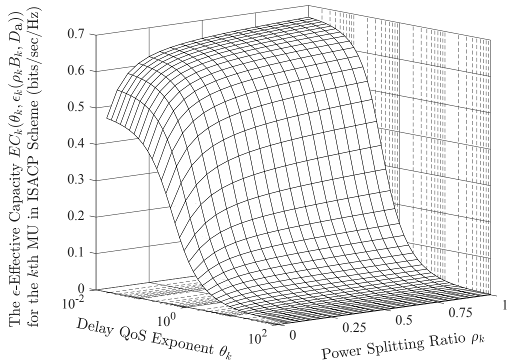

Fig. 4. The ϵ-effective capacity in our proposed ISACP scheme under different values of delay QoS exponent θ_k and power splitting ratio ρ_k for the kth MU.

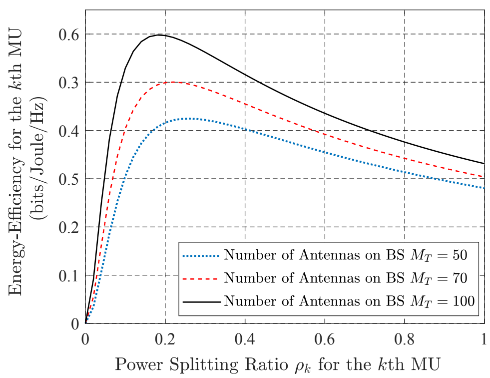

Fig. 5. Energy-efficiency under different values of the number of antennas M_T on the massive MIMO BS and power splitting ratio ρ_k for the kth MU.

increasing function of the power splitting ratio ρ_k. However, if ρ_k is larger than 0.2, the ϵ-effective capacity increases slowly as ρ_k further increases, showing that a larger power for the sensing and communication signal cannot achieve a significant improvement for the communication performance.

Figure 5 plots the kth MU's energy-efficiency under different values of the number of antennas M_T on the massive MIMO BS and power splitting ratio ρ_k. Figure 5 reveals that there always exists the optimal ρ_k for the kth MU to maximize its energy-efficiency, and thus, there exists the optimal vector $\boldsymbol{\rho}$ for all MUs, to maximize the overall energy-efficiency $\eta(\boldsymbol{\rho})$ given by Eq. (18). In Fig. 5, the maximum energy-efficiency increases as the number of massive MIMO antennas M_T increases, showing that a larger M_T can improve the performance for our ISACP schemes. We also observe from Fig. 5 that the optimal power splitting ratio ρ_k decreases as M_T increases, showing that the sensing and communication signal requires a smaller power allocation if the BS is equipped with more antennas. Thus, using a larger M_T on the BS can not only deliver more power to the energy harvesting device, but also improve the energy-efficiency of the wireless networks.

Figure 6 plots the decoding error probability $\epsilon_k(\rho_k B_k, D_\mathrm{a})$ against different values of power splitting ratio ρ_k for the kth MU. Figure 6 reveals that the decoding error probability $\epsilon_k(\rho_k B_k, D_\mathrm{a})$ monotonically decreases as the power splitting ratio ρ_k and the number of antennas M_T on BS increase, and $\epsilon_k(\rho_k B_k, D_\mathrm{a})$ decreases with a slower rate if the power

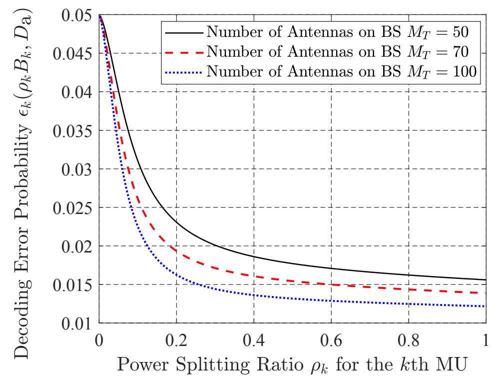

Fig. 6. The decoding error probability $\epsilon_k(\rho_k B_k, D_\mathrm{a})$ in our proposed ISACP scheme under different values of power splitting ratio ρ_k for the kth MU.

splitting ratio ρ_k is larger than 0.4. Thus, Figs. 3-6 indicate that the power splitting ratio ρ_k can be selected in the range of [0.2, 0.4] to achieve the optimal performances for our proposed ISACP schemes.

VI. Conclusions

To support the mURLLC traffic over the 6G wireless networks, we have proposed the ISACP schemes to integrate the ISAC with the SWIPT techniques to simultaneously sense the wireless channel, and wirelessly transfer the information and power. We have developed the Cramér-Rao bound, channel state estimation distortion, and capacity-distortion function to measure the radar sensing, channel estimation, and communication performances, respectively. We have also proposed to apply the ϵ-effective capacity to support both statistical delay and error-rate bounded QoS provisioning for the mURLLC traffic over 6G. By optimizing the power splitting ratio between the ISAC signal power and energy harvesting, we have achieved the maximum energy-efficiency for ISACP schemes.

References

[1] Z. He, W. Xu, H. Shen, D. W. K. Ng, Y. C. Eldar, and X. You, "Full-duplex communication for ISAC: Joint beamforming and power optimization," *IEEE Journal on Selected Areas in Communications*, vol. 41, no. 9, pp. 2920–2936, 2023.

[2] M. Liu, M. Yang, H. Li, K. Zeng, Z. Zhang, A. Nallanathan, G. Wang, and L. Hanzo, "Performance analysis and power allocation for cooperative ISAC networks," *IEEE Internet of Things Journal*, vol. 10, no. 7, pp. 6336–6351, 2023.

[3] H. Liu and E. Alsusa, "A novel ISaC approach for uplink NOMA system," *IEEE Communications Letters*, vol. 27, no. 9, pp. 2333–2337, 2023.

[4] S. M. Kay, *Fundamentals of Statistical Signal Processing: Estimation Theory*. Prentice-Hall, Inc., 1993.

[5] I. Bekkerman and J. Tabrikian, "Target detection and localization using MIMO radars and sonars," *IEEE Transactions on Signal Processing*, vol. 54, no. 10, pp. 3873–3883, 2006.

[6] Y. Polyanskiy, H. V. Poor, and S. Verdú, "Channel coding rate in the finite blocklength regime," *IEEE Transactions on Information Theory*, vol. 56, no. 5, pp. 2307–2359, 2010.

[7] M. Kobayashi, G. Caire, and G. Kramer, "Joint state sensing and communication: Optimal tradeoff for a memoryless case," in *Proc. IEEE ISIT 2018*, pp. 111–115.

[8] J. Tang and X. Zhang, "Quality-of-service driven power and rate adaptation over wireless links," *IEEE Transactions on Wireless Communications*, vol. 6, no. 8, pp. 3058–3068, Aug. 2007.

[9] X. Zhang, J. Tang, H.-H. Chen, and S. Ci, "Cross-layer-based modeling for quality of service guarantees in mobile wireless networks," *IEEE Communications Magazine*, vol. 44, no. 1, pp. 100–106, 2006.